12,11

Structural transition and temperature dependencies of thermal expansion coefficients of $NaNO_3$ embedded into the nanoporous glass

© A.A. Naberezhnov[1], O.A. Alekseeva[2], A.V. Kudriavtzeva[2], D.Yu. Chernyshov[2,3], T.Yu. Vergentiev[4], A.V. Fokin[1]

[1] Ioffe Institute,
St. Petersburg, Russia
[2] Peter the Great Saint-Petersburg Polytechnic University,
St. Petersburg, Russia
[3] European Synchrotron Radiation Facility,
Grenoble, France
[4] OJSC „Morion“,
St. Petersburg, Russia

E-mail: alex.nabereznov@mail.ioffe.ru

Received November 11, 2021
Revised November 11, 2021
Accepted November 13, 2021

The temperature evolution of the crystal structure of a nanocomposite material obtained by introducing sodium nitrate $NaNO_3$ from a melt under pressure into a nanoporous alkali borosilicate glass with an average pore diameter of 7 nm has been studied by the method of diffraction of synchrotron radiation in a wide temperature range upon heating. Analysis of the experimental diffraction patterns revealed a significant decrease in the temperature of the structural (orientational) transition by more than 50 K (up to 496 K) compared to bulk sodium nitrate. From the temperature dependence of the intensity of the superstructure peak (113), the dependence of the critical exponent $\beta(T)$ for this transition was obtained and a significant difference from the critical exponent for a bulk material was found in the temperature range from 455 K to the transition temperature. Analysis of the broadening of Bragg reflections made it possible to estimate the average size (~ 40 nm) of sodium nitrate nanoparticles into the pores. An increase in the linear coefficient of thermal expansion in the [001] direction was found in NaNO3 nanoparticles in comparison with bulk material at temperatures above 450 K.

Keywords: porous glasses, phase transitions, nanocomposite materials, synchrotron radiation diffraction, sodium nitrate, restricted geometry, structure, size effects.

DOI: 10.21883/PSS.2022.03.53192.239

1. Introduction

The physical properties of systems consisting of ultrasmall particles, phase transitions, and the critical phenomena occurring in them have been intensively studied in recent decades. Nanocomposite materials (NCM) based on them can exhibit unusual electronic, thermal, structural, optical and other properties and be used to create new electronic devices and/or expand the functional characteristics of existing ones. The main reasons for the differences in the physical properties of NCM from those for the massive substance on the physical properties of nanoobjects with the decrease in their characteristic sizes are the closeness of the values of the lengths of characteristic interactions and sizes of nanoparticles, as well as an increase in the influence of surface atoms (for which local symmetry and interaction with the matrix walls and the environment are significantly different from internal atoms).

One of the NCM fabrication methods is the incorporation (or synthesis) of substances into nanosized pores of the porous matrix. As the porous matrix, porous glass, chrysotile asbestos, artificial opals, zeolites, mesoporous matrices MCM-41 and SBA-15 [1–3] can be used. In our work, for the manufacture of NCM, we used alkali-borosilicate porous glass (ABG) with an average pore diameter of 7 nm. In these glasses, after special heat treatment, phase separation into two components occurs: a stable phase consisting of amorphous SiO_2, which forms the framework of this matrix, and a chemically unstable alkali-borate phase [4]. By selecting the heat treatment conditions and varying the initial composition of the mixture, it is possible to form the system of these two interpenetrating phases [5]. After chemical etching of these glasses, a 3D-structure is formed, which can be defined as a through disordered dendritic structure of an empty pore space penetrating the frame of an amorphous silica matrix. Pores in glasses are interconnected and their average diameter has the small spread (in our case $\sim 5-10\%$). Depending on the preparation conditions, the average pore diameter can vary from 20–30 Å to tens of nanometers. The typical example of a porous silicate glass is the industrial glass of the Vycor type [1]. Standard chemical composition: 96% SiO_2, 3% B_2O_3, 0.40% Na_2O, R_2O_3 or $RO_2 < 1\%$ (in preference Al_2O_3 and ZrO_2) [6].

In NCMs based on porous media filled with various ferroelectrics, the giant increase in the permittivity in the

paraelectric phase [7–12], the change in the parameters of the phase transition and the type of phase transition [13–17], the stabilization of metastable phases [18–20], and the existence of critical sizes of nanoparticles [13,18] were detected.

Massive sodium nitrate $NaNO_3$ undergoes an orientational (structural) phase transition „order–disorder" at a temperature of 549 K and melts at $T \sim 580$ K. At low temperature, it crystallizes in the calcite structure (spatial group R-3c) with two formula units per unit cell, the dimensions of which are $a = b = 5.075$ Å, $c = 17.07$ Å [21]. Unlike $NaNO_2$, no ferroelectric phase is formed. Upon heating, the gradual orientational disordering of nitrate molecular groups NO_3 around the threefold axis parallel to the crystallographic axis c occurs, and at the temperature of 549 K, the structural transition R-3c → R-3m occurs. It is accompanied by the disappearance of superstructural reflections at points Z of the reciprocal space, that is, at the point (0 0 1.5) indexed using the hexagonal setting R-3m. The intensity of superstructural peaks obeys the power law $I = I_0\tau^{\beta}$, where τ is the reduced temperature: $\tau = (T_c - T)/T_c$, β is the critical index.

In massive sodium nitrate $NaNO_3$, the β index exhibits complex behavior upon heating. In the wide temperature range (280−460 K) its value is $\beta = 0.25$ [22], then in the temperature range of 460−543 K the value β decreases to 0.22 and then sharply increases to 0.41 in the vicinity of the orientational transition [23].

Dielectric studies have shown that in nanostructured sodium nitrate, when approaching the melting temperature, there is the sharp increase in the dielectric constant (as in $NaNO_2$) [24]. The results of differential scanning calorimetry (DSC) showed that in NCM based on porous glasses with average pore diameter of 320 nm and 46 nm containing $NaNO_3$, with the decrease in the pore diameter, the melting temperature decreases, the tailing of the orientational structural transition and the shift of the corresponding heat capacity maximum $C_P(T)$ towards lower temperatures. In [25] by DSC and Raman spectroscopy for NCM ($NaNO_3$ + porous glass) with average pore radius of 2.5, 5, 10, and 20 nm, suppression of the phase transition „melting−solidification" were found for NCM with a glass pore size of 2.5 nm and the appearance of a new $NaNO_3$ phase in NCM based on glasses with pore diameters of 5, 10 and 20 nm, stabilized by hydroxyl OH-groups and adsorbed water on the silica surface and characterized by the appearance of a new transverse optical mode, which is not observed in the spectrum of massive $NaNO_3$.

Thus, it has been established that $NaNO_3$ exhibits unusual physical properties under conditions of limited geometry, however, detailed studies of the temperature evolution of the ($NaNO_3$ + NCM,porous glass) structure with the ultrasmall pore size NCM have not previously been carried out (in the work [26] the results for NCM ($NaNO_3$ + porous glass) 320 (PG320) and 46 nm (PG46) are given, but for PG7 sufficient statistics are not obtained). Moreover, the temperature dependences of $\beta(T)$ and the transition temperature were obtained only for NCMs based on PG320 and PG46, while the data for PG7 only allowed us to estimate T_C. The value of the critical index for NCM ($NaNO_3$ + PG46) $\beta = 0.16(3)$ was obtained, which is somewhat less compared to bulk material, and for NCM ($NaNO_3$ + PG320) $\beta = 0.31(2)$, i.e., some increase in comparison with the array was observed, apparently associated with the presence of texture in the sample. It has been established that for NCM ($NaNO_3$ + PG320) the orientational transition temperature does not differ from the array and is $T_c = 551$ K, for NCM ($NaNO_3$ + PG46) and ($NaNO_3$ + PG7) T_c decreases and amounts to 531 and 497 K respectively.

The main goal of this work was to obtain information on the evolution of the crystal structure, to obtain the dependence of the critical index $\beta(T)$, as well as the thermal expansion coefficients in NCM ($NaNO_3$ + porous glass) 7 nm in a wide temperature range during heating, including the region of orientational transition.

2. Sample preparation and experiment procedure

Porous glass was obtained by etching alkaline-borosilicate glass. The obtained porous glasses contained about 90% of SiO_2. The average pore diameter was determined by adsorption poroscopy and mercury porosimetry and amounted to 7(1) nm. The porosity, determined by the method of mass reduction after leaching, was found to be 23%. $NaNO_3$ was introduced into the porous glass from the melt under pressure. According to the results of the analysis of the change in the weight of the samples, the degree of filling of the pore space was about 90%. After filling pores, the surfaces of the plates were mechanically cleaned to remove the remnants of massive $NaNO_3$.

The study of the temperature evolution of the structure was carried out during heating in the temperature range of 300−600 K by the method of synchrotron radiation diffraction (station BM01A, ESRF, France) at the wavelength $\lambda = 0.703434$ Å. The temperature step was 2 K, and the temperature stabilization was no worse than 1 K. The results obtained were processed by the Rietveld full-profile analysis in the FullProf software environment.

3. Results and discussion

Figure 1 shows typical diffraction spectra at two temperatures and the results of their fitting in the FullProf program. The positions of all Bragg reflections correspond to the $NaNO_3$ structure; no foreign impurities or phases were found. The large background value is associated with scattering on the amorphous framework of the matrix. Vertical dashes indicate superstructural peaks (113) and (211), which, as can be seen, are absent in the diffraction pattern obtained at $T = 505$ K.

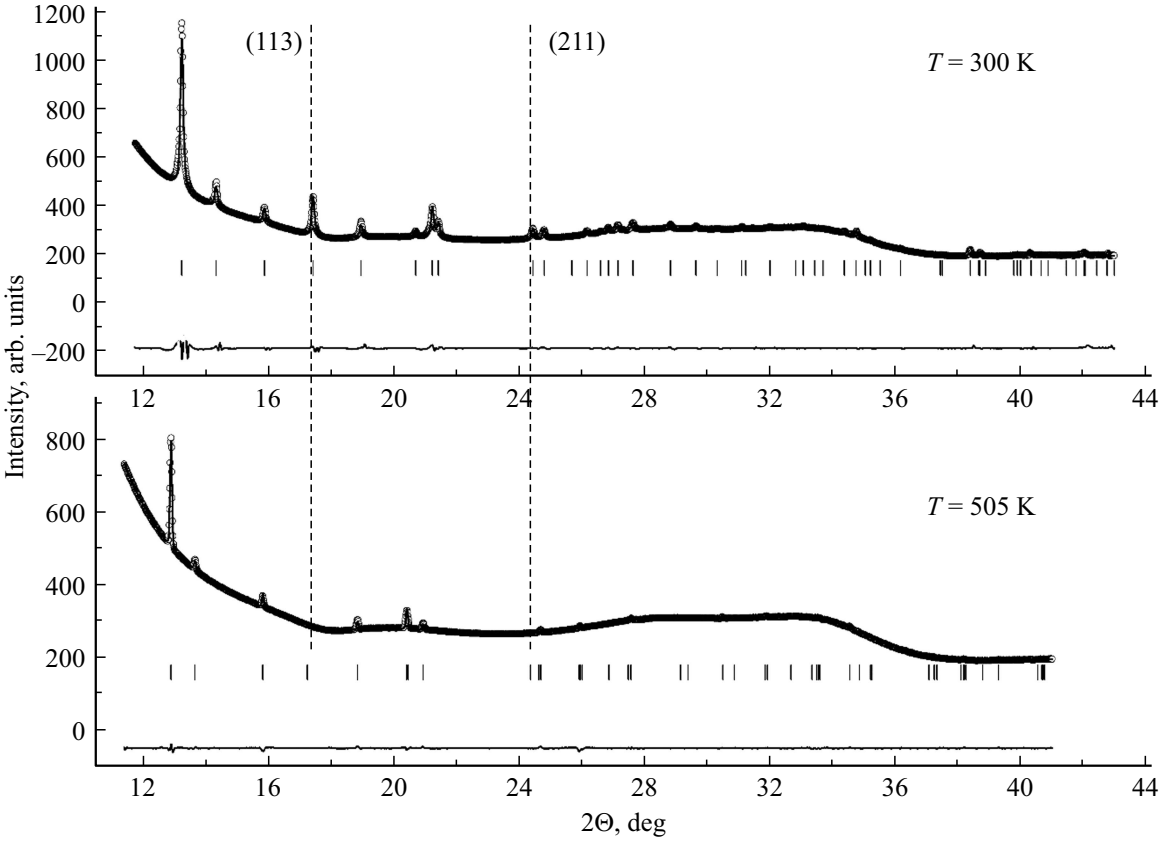

Figure 1. Diffraction spectra for NCM ($NaNO_3 + PG7$) at temperatures of 300 and 505 K. The lines at the bottom of each diffractogram — discrepancy between the experimental spectrum and processing. Vertical dashes — positions of elastic peaks for $NaNO_3$. Points and lines passing through them — experimental data and processing results, respectively. The vertical dotted lines indicate the positions of the superstructural peaks (113) and (211).

The temperature dependence of the intensity of the superstructural peak (113) (Fig. 2) at the temperature of approximately $T^* \sim 455$ K shows the kink. Approximation of two sections of the dependence above and below this temperature by the power function $I = I_0\tau^\beta$, where τ — reduced temperature $\tau = (T_c - T)/T_c$, β — critical index, gives the following values of the critical index $\beta_{T<T^*} = 0.25(2)$ and $\beta_{T>T^*} = 0.48(3)$. Thus, a crossover of the temperature behavior of the critical index is observed at the temperature $T^* \sim 455$ K.

Thus, below the crossover temperature T^*, the value β obtained by us coincides with the value for massive $NaNO_3$, and above T^* it exceeds it by more than 2 times. Approximation of the region above the crossover temperature gives the value of the structural transition temperature $T_c = 496(1)$ K, which is much lower T_c for massive $NaNO_3$, which is 549 K. The value T_c obtained by us in this work for the NCM ($NaNO_3 + PG7$) is in good agreement with the value $T_c = 497$ K [26] obtained from the analysis of the neutron diffraction on NCM ($NaNO_3 + PG7$), which was prepared by introducing sodium nitrate into the pores of PG7 from an aqueous solution.

The Bragg peaks in all X-ray diffraction patterns are clearly broadened compared to the instrumental linewidth due to the size effect. Using profile analysis, we also plotted the temperature dependence of the sizes of $NaNO_3$ nanoparticles in this NCM (Fig. 3). At room temperature, the average particle size is 40(5) nm, which is several times greater than the average pore diameter 7 nm and is due to the fact that when the matrix is filled with the introduced substance, the nanoparticle is formed in several adjacent channels of the pore space. The average size of nanoparticles remains unchanged in the wide temperature range up to temperatures on the order of 450 K, above which the significant increase in size begins with further heating.

This increase can be associated with size-induced melting point of $NaNO_3$ nanoparticles, as a result of which the main contribution to the intensity of elastic peaks begins to come from the remains of the massive phase contained in the sample, which lead to the sharp increase in the observed diffraction size of particles. The second reason may be the merging of neighboring particles into larger due to their expansion upon heating. The combination of these mechanisms is also possible. Unfortunately, it is currently not possible to separate them.

In parallel, from data processing, we obtained the temperature dependences of the cell parameters and calculated

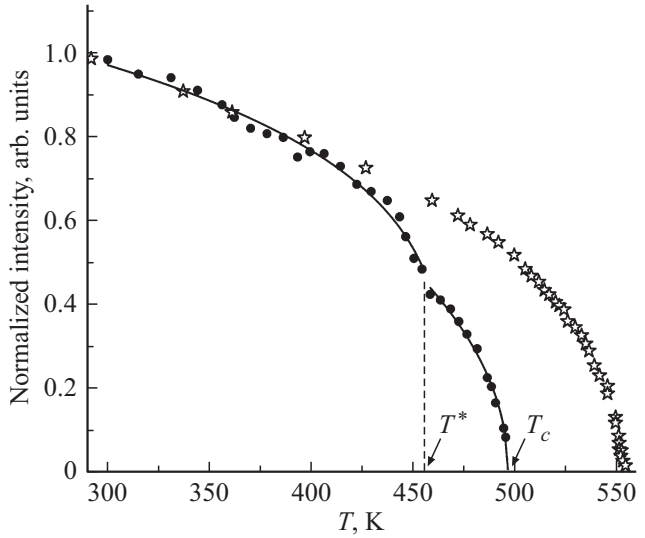

Figure 2. Temperature dependence of the normalized intensity of the superstructural peak (113) (points) and approximation of its segments above and below $T = 455\,\mathrm{K}$ by the power function $I = I_0\tau^{\beta}$ (lines). The asterisks indicate the points of the temperature dependence of the peak intensity of the superstructural peak of massive $NaNO_3$ taken from the paper [27].

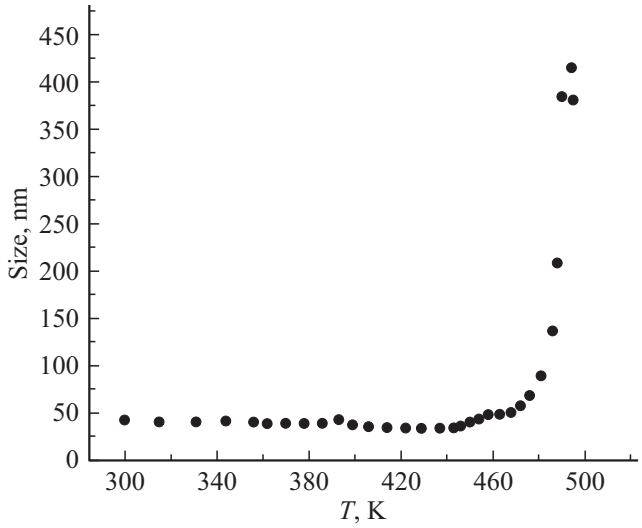

Figure 3. Temperature dependence of the sizes of nanoparticles of sodium nitrate $NaNO_3$ in porous glass PG7. The error does not exceed the symbols size.

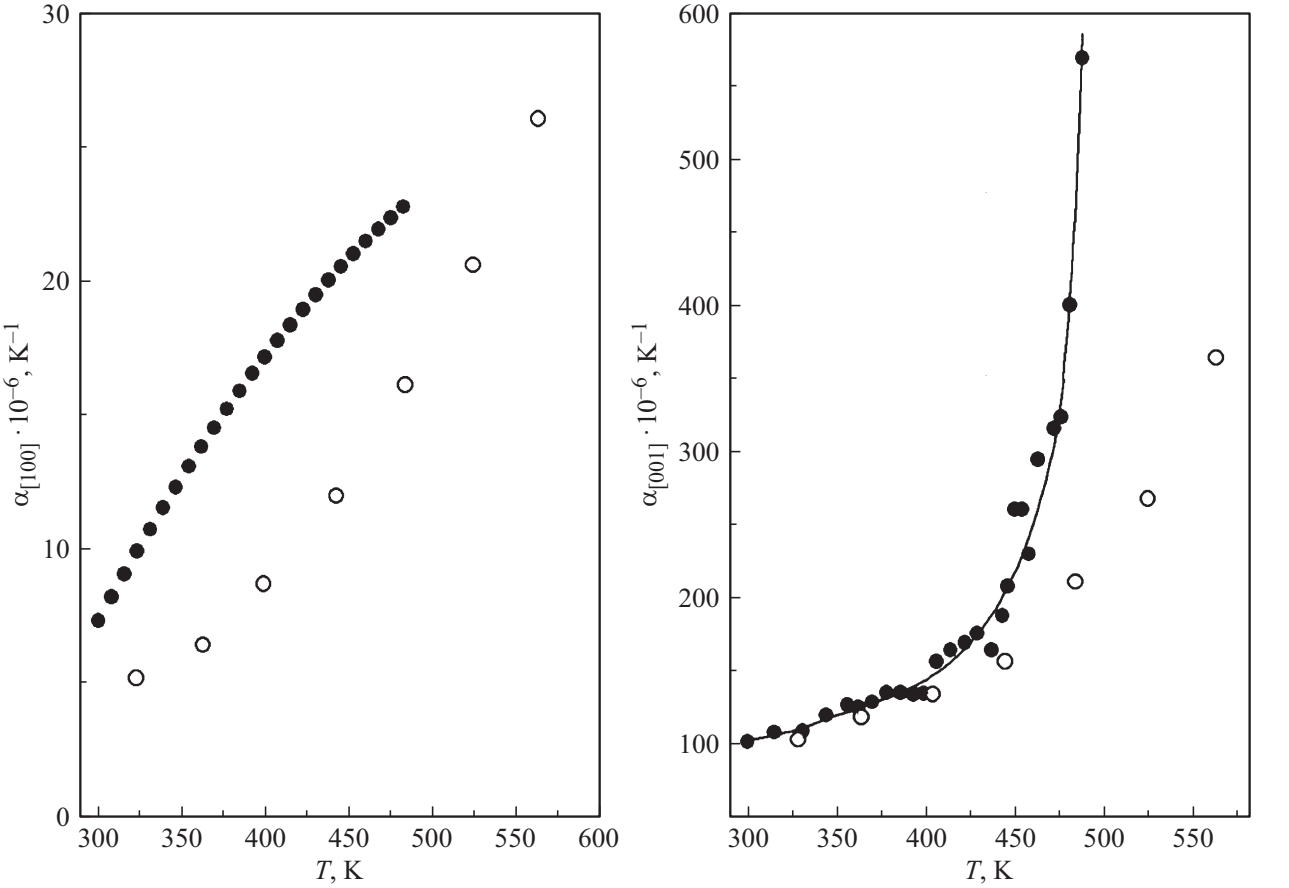

Figure 4. Temperature dependences of the linear coefficients of thermal expansion α along the directions [100] and [001] for NCM ($NaNO_3$ + PG7) (black circles) and for massive $NaNO_3$ [28] (white circles).

the values of linear thermal expansion coefficients α (TEC) along the directions [100] and [001] (black dots in Fig. 4). For comparison, the figure also shows the values for the massive material (white circles — from data of the work [28]).

It can be seen from Fig. 4 that along the direction [001], at temperatures above about 450 K, there is the sharp increase in TEC compared to massive $NaNO_3$, and along the direction [100], there is the difference in α values for a nanostructured and massive $NaNO_3$, but not so significant.

It should be noted that the revealed features of the temperature behavior of the TEC, nanoparticle size, and critical index begin to manifest themselves at temperatures above ~ 450 K and can be associated with the observed crossover in the behavior of the critical index $\beta(T)$. In the future, by analogy with the works [29,30] carried out for $NaNO_2$ NCMs in porous glasses, we plan to study the temperature dependences of the amplitudes of thermal vibrations of $NaNO_3$ atoms in NCM ($NaNO_3 + PG7$), which may help explain the origin of the observed anomalies precisely at this temperature.

4. Conclusion

Diffraction studies of the temperature evolution of the crystal structure of $NaNO_3$ nanoparticles embedded in PG7 nanoporous glass upon heating in the temperature range of 300−600 K have been carried out. The temperature dependence of the average size of $NaNO_3$ nanoparticles is obtained, which at room temperature is $\sim 40(5)$ nm. From the approximation of the temperature dependence of the intensity of the superstructural peak (113), the temperature of the structural orientational transition was determined, which in this NCM is 496(1) K, which is more than 50 K lower than in massive sodium nitrate. The temperature dependence of the critical index $\beta(T)$ is obtained and the existence of a crossover behavior of $\beta(T)$ near $T^* \sim 455$ K is established. The significant increase in the linear coefficient of thermal expansion along the direction [001] in nanoparticles compared to massive material at temperatures above 450 K is established.

Funding

In the Peter the Great Saint Petersburg Polytechnic University the works has been partially funded by the Russian Foundation for Basic Research (BRICS grant No. 19-52-80019).

D.Yu. Chernyshov is grateful to the RFBR grant 19-29-12023 for partial financial support during the research.

Conflict of interest

The authors declare that they have no conflict of interest.

References

[1] P. Levitz, G. Ehret, S. K. Sinha, J. M. Drake. J. Chem. Phys. **95**, *8*, 6151 (1991).
[2] F.L. Pundsack. J. Phys. Chem. **65**, *1*, 30 (1961)
[3] D.W. Breck. Zeolite molecular sieves. A Willey-Interscience Publication Jonh Willey & Sons, N.Y. (1974). p. 771.
[4] O.V. Mazurin, G.P. Roskova, V.I. Aver'yanov. Two-phase glasses: structure, properties, application. Nauka, L. (1991). 276 p.
[5] T.N. Vasilevskaya, T.V. Antropova. Physics of the Solid State **51**, *12*, 2386 (2009).
[6] X. Huang. J. Non-Cryst. Solids **112**, *1–3*, 58 (1989).
[7] E.V. Colla, E.Yu. Koroleva, Yu.A. Kumzerov, B.N. Savenko, S.B. Vakhrushev. Ferroelectr. Lett. **20**, *5–6*, 143 (1996).
[8] E. Koroleva, A. Naberezhnov, E. Rysiakiewicz-Pasek, S. Vakhrushev, A. Sysoeva, Yu. Kumzerov. Composites B **94**, *1*, 322 (2016).
[9] M. Kinka, J. Banys, A. Naberezhnov. Ferroelectrics **348**, *1*, 67 (2007).
[10] S.V. Baryshnikov, E.V. Charnaya, Yu.A. Shatskaya, A.Yu. Milinsky, M.I. Samoilovich. Physics of the Solid State **53**, *6*, 1146 (2011).
[11] E.V. Colla, A. V. Fokin, Y. A. Kumzerov. Solid State Commun. **103**, *2*, 127 (1997).
[12] O.V. Rogazinskaya, S.D. Milovidova, A.S. Sidorkin, N.G. Popravko, M. A. Bosykh, V.S. Enshina. Ferroelectrics **397**, *1*, 191 (2010).
[13] A. Fokin, Yu. Kumzerov, E. Koroleva, A. Naberezhnov, O. Smirnov, M. Tovar, S. Vakhrushev, M. Glazman. J. Electroceram. **22**, *1–3*, 270 (2009).
[14] P.Y. Vanina, A.A. Naberezhnov, O.A. Alekseeva, A.A. Sysoeva, D.P. Danilovich, V.I. Nizhankovskii. Nanosystems: Phys. Chem. Math. **8**, *4*, 535 (2017).
[15] A. Sieradzki, J. Komar, E. Rysiakiewicz-Pasek, A. Ciżman, R. Poprawski. Ferroelectrics 402, *1*, 60 (2010).
[16] A.I. Beskrovny, S.G. Vasilovsky, S.B. Vakhrushev, D.A. Kurdyukov, O.I. Zvorykina, A.A. Naberezhnov, N.M. Okuneva. Physics of the Solid State **52**, *5*, 1021 (2010).
[17] R. Poprawski, E.Rysiakiewicz-Pasek, A.Sieradzki, A.Ciżman, J. Polańska. J. Non-Cryst. Solids **353**, *47–51*, 4457 (2007).
[18] A.A. Naberezhnov, P.Yu. Vanina, A.A. Sysoeva. Physics of the Solid State **60**, *3*, 439 (2018).
[19] B. Dorner, I. Golosovsky, Yu. Kumzerov, D. Kurdyukov, A. Naberezhnov, A. Sotnikov. Ferroelectrics **286**, *1*, 213 (2003).
[20] S.V. Baryshnikov, E.V. Charnay, A.Yu. Milinskiy, Yu.A. Shatskaya, Cheng Tien, D. Michel. Physica B **405**, *16*, 3299 (2010).
[21] P. Cherin, W.C. Hamilton, B. Post. Acta Crystallographica **23**, *3*, 455 (1967).
[22] W.W. Schmahl, E. Salje. Phys Chem. Minerals **16**, *8*, 790 (1989).
[23] W.C.-K. Poon, E. Salje. J. Phys. C **21**, *4*, 715 (1988).
[24] A.S. Balabinskaya, E.N. Ivanova, M.S. Ivanova, Yu.A. Kumzerov, S.V. Pan'kova, V.V. Poborchii, S.G. Romanov, V.G. Soloviev, S.D. Khanin. Fizika i khimiya stekla **31**, *3*, 440 (2005) (in Russian).
[25] R. Mu, F. Jin, S.H. Morgan, D.O. Henderson, E. Silberman, J. Chem. Phys. **100**, *10*, 7749 (1994).
[26] E. Rysiakiewicz-Pasek, A. Naberezhnov, M. Seregin, E. Koroleva, I. Glavatskyy, M. Tovar, A. Sysoeva, E. Berman. J. Non-Crystall. Solids **357**, *14*, 2580 (2011).

[27] S.J. Payne, M.J. Harris, M.E. Hagen, M.T. Dove. J. Phys. Condens. Matter **9**, *11*, 2423 (1997).
[28] K.V. Krishna Rao, K. Satyanarayana Murthy. J. Phys. Chem. Solids **31**, *4*, 887 (1970).
[29] A.V. Fokin, Yu.A. Kumzerov, A.A. Naberezhnov, N.M. Okuneva, S.B. Vakhrushev, I.V. Golosovsky, A.I. Kurbakov. Phys. Rev. Lett. **89**, *17*, 175503-1 (2002).
[30] A. Beskrovny, I. Golosovsky, A.Fokin, Yu. Kumzerov, A. Kurbakov, A. Naberezhnov, S. Vakhrushev. Appl. Phys. A **74**, supplement issue 1, s1001 (2002).